Spatially-resolved line emission from radiation-hydrodynamics simulations

Aaron Smith (CfA)

Heidelberg-Harvard

December 6, 2022

CENTER FOR ASTROPHYSICS HARVARD & SMITHSONIAN

Emission Lines: Sandro Tacchella + Rahul Kannan + SMUGGLE Team

Thesan: Rahul Kannan, Enrico Garaldi, Mark Vogelsberger, Rüdiger Pakmor, Volker Springel, Lars Hernquist

Extensions: Ewald Puchwein, Laura Keating, Josh Borrow, Federico Marinacci, Jessica Yeh, Clara Xu, Meredith Neyer

Hydrogen Emission Lines

- ★ Ionizing radiation from stars is efficiently converted to recombination line emission
- ★ Lyman-alpha emitting galaxies (LAEs) are observed out to z~10 (high-z frontier)
- ★ H-alpha maps star formation on spatially resolved scales in galaxies out to z~3
- ★ Breakthroughs due to integral field units at 10m facilities (e.g. MANGA, MUSE, KCWI)
- ★ Spatially and spectrally resolved studies are increasingly common in observations

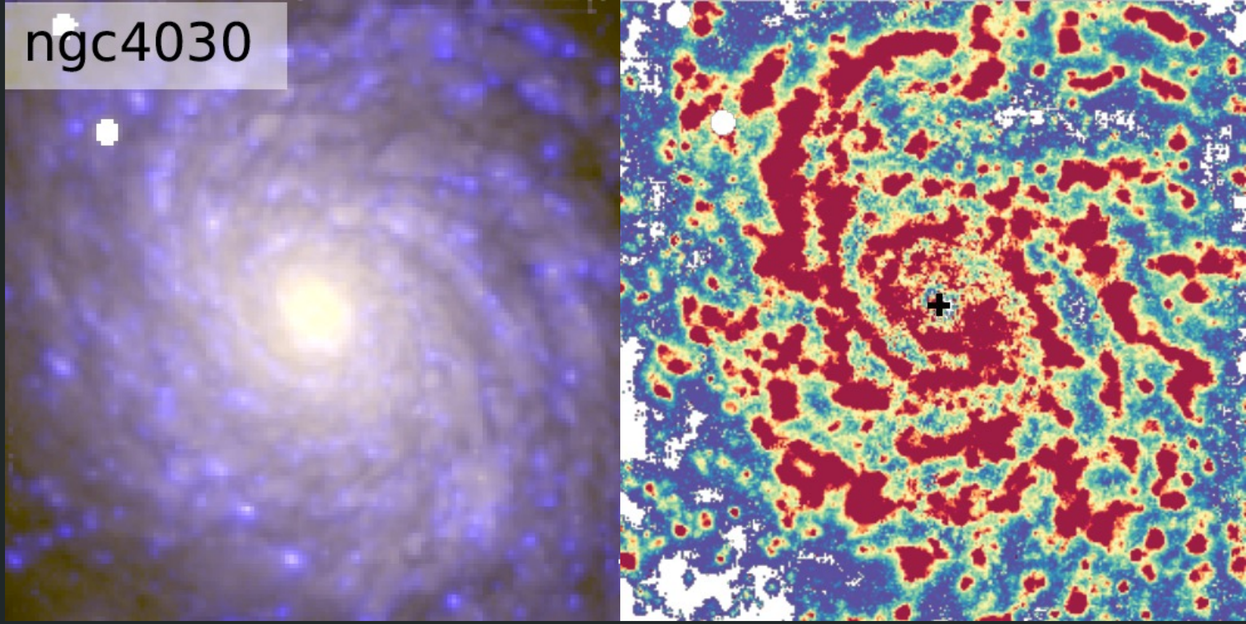

H-alpha – Erroz-Ferrer et al. (2019)

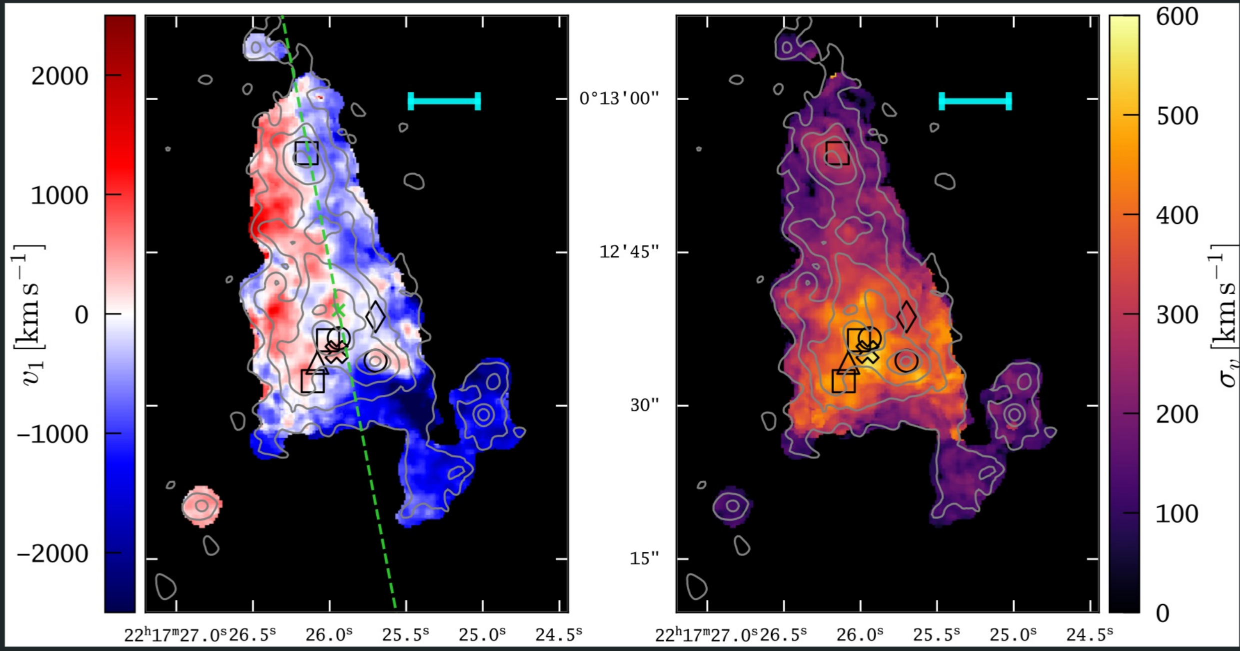

Lyman-alpha – Herenz et al. (2020)

But isn't H-alpha trivial?

★ Numerous complications for ionization:
- Pre-absorption of LyC photons by dust
- Account for helium/metal ionization
- Uncertain LyC escape fractions
- Extraplanar/extragalactic radiation
- Scattering, collisions, shocks, AGN, etc.
- Old stars, diffuse ionized gas (DIG), etc.

★ Additional complications for lines:
- Recombination + collisional excitation
- Uncertain dust properties + extinction
- Complex geometry + anisotropic escape
- Note: Lyα also has resonant scattering

★ These bias SFR, dust, metallicity estimates

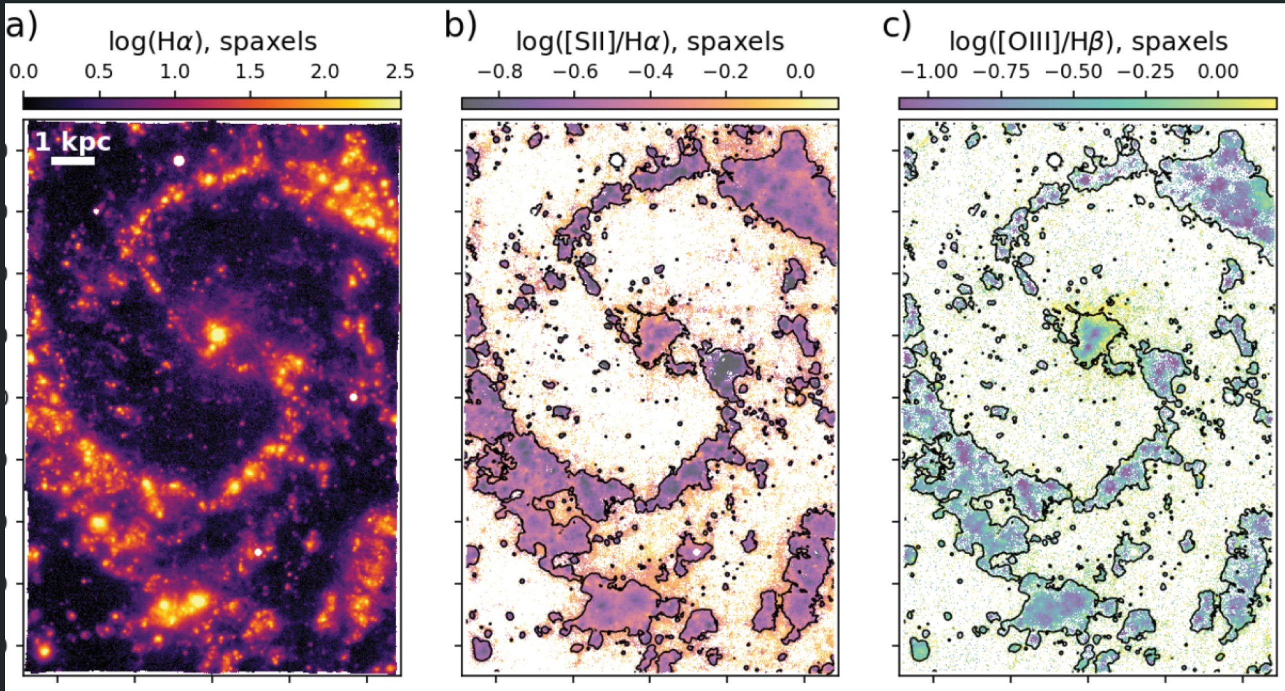

DIG/BTP – Belfiore et al. (2022)

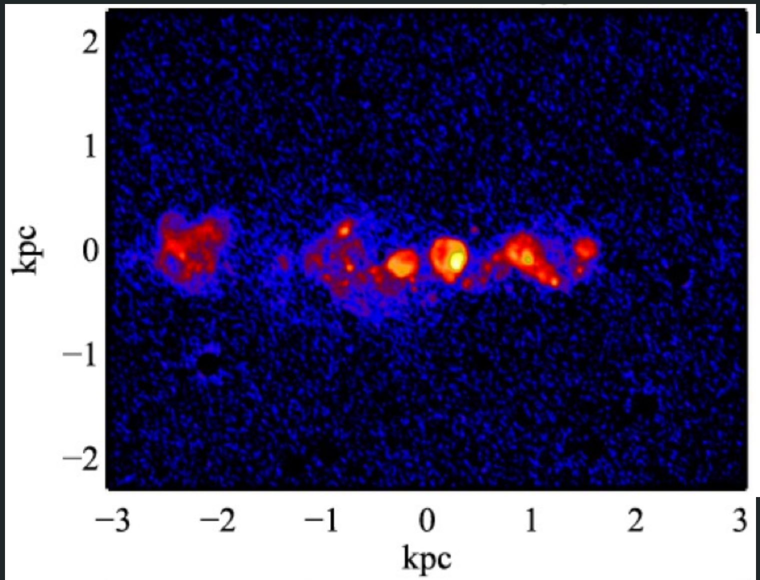

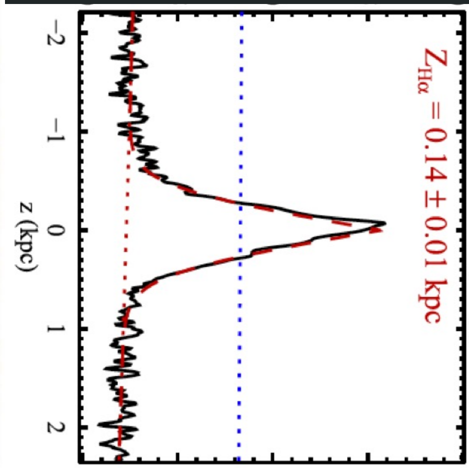

Jo et al. (2018)

Schema for H-alpha Radiative Transfer

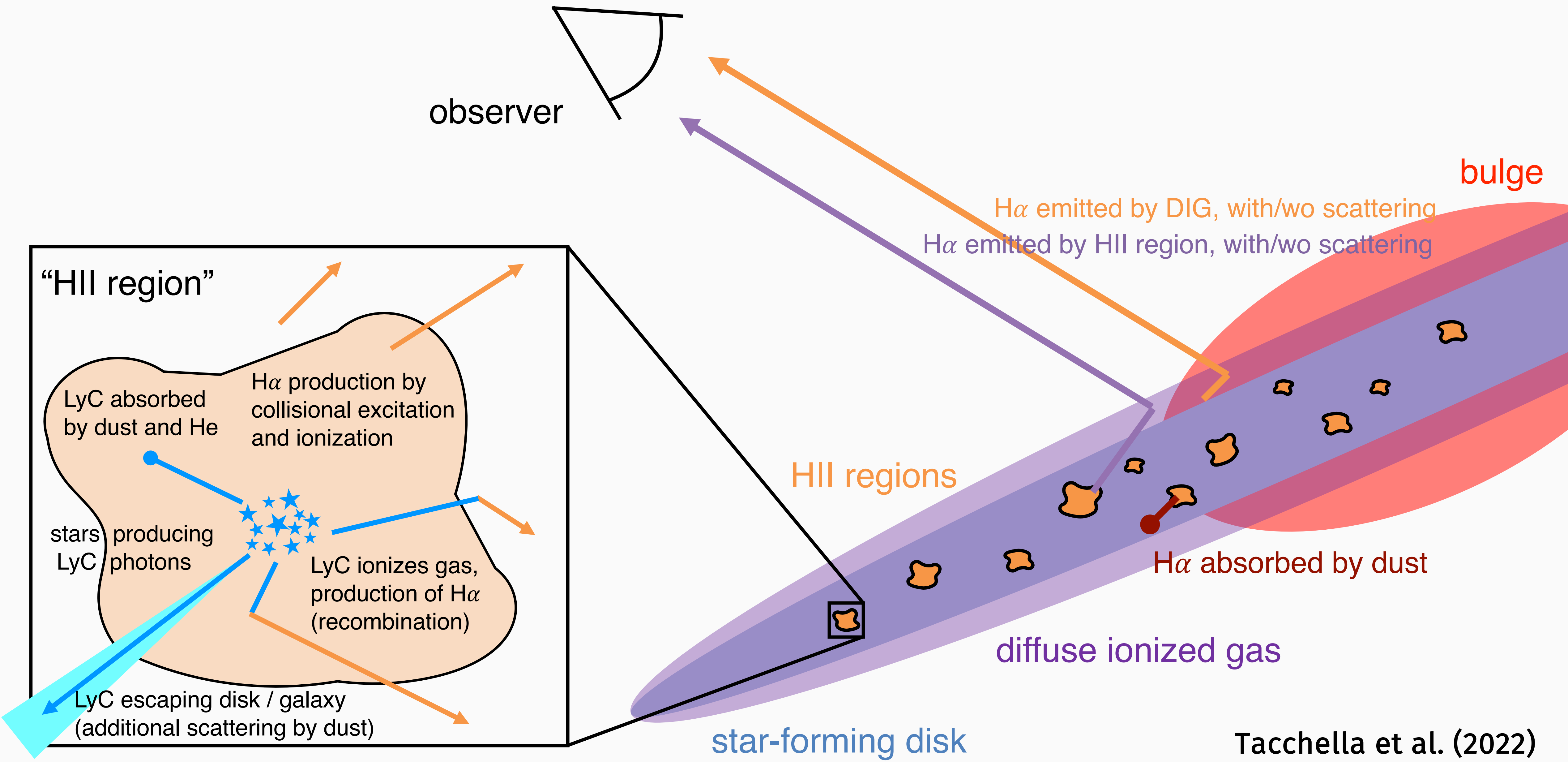

Isolated disk simulations

★ Based on Kannan et al. (2020, 2021)
- Arepo-RT – M1 RHD solver
- SMUGGLE sub-grid model
- RT captures radiation pressure, photoheating, etc. (BC03)
- Self-consistent dust model
- Resolution: $m_{gas} = 1.4 \times 10^3\ M_\odot$
- Softening: 3.6 pc (gas)
- Run for 1 Gyr

M_{halo} $[M_\odot]$	$M_\star$ $[M_\odot]$	M_{gas} $[M_\odot]$	SFR $[M_\odot\,\mathrm{yr}^{-1}]$
1.5×10^{12}	6.2×10^{10}	4.2×10^{9}	2.7

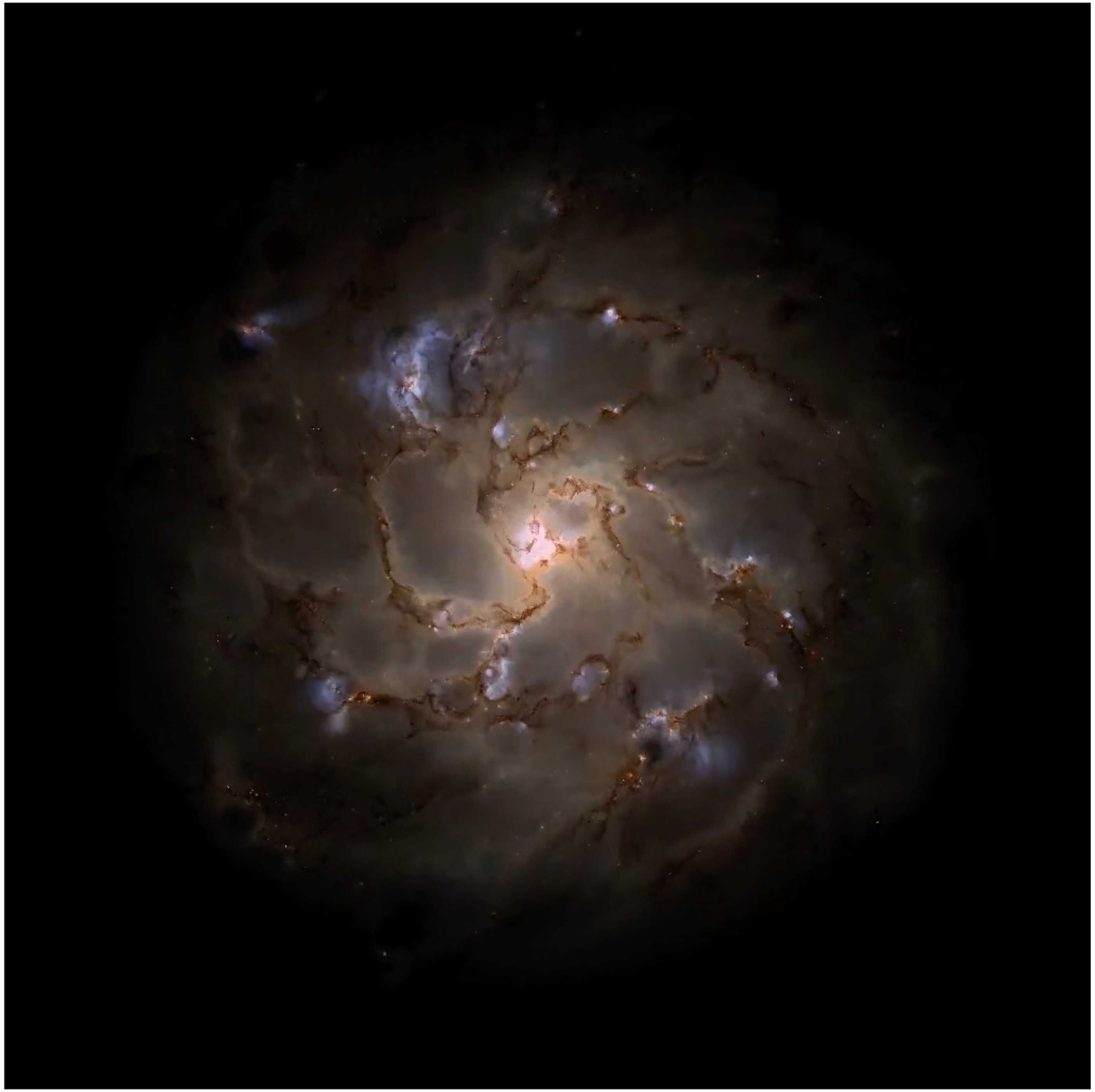

Under-resolved HII regions: need for post-processing

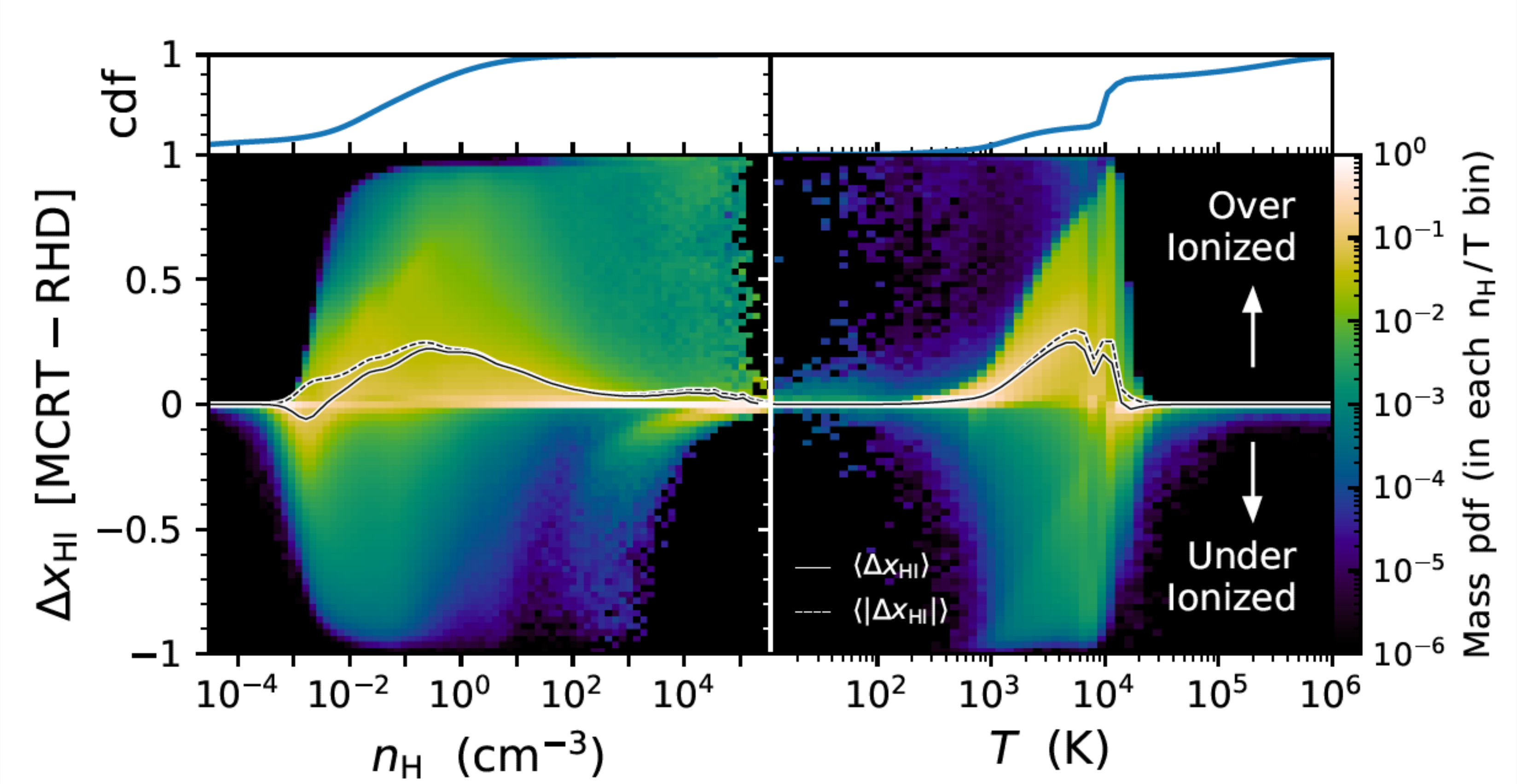

- On-the-fly radiation-hydrodynamic simulations under-resolve HII regions
  (high-density gas is over-ionized, leading to an over-prediction of recombination emission)
- We solve this problem by performing MCRT in post-processing
  (retain the gas internal energy as this is already faithfully modeled but we iteratively recalculate the ionizing radiation field and update the ionization states assuming photoionization equilibrium)

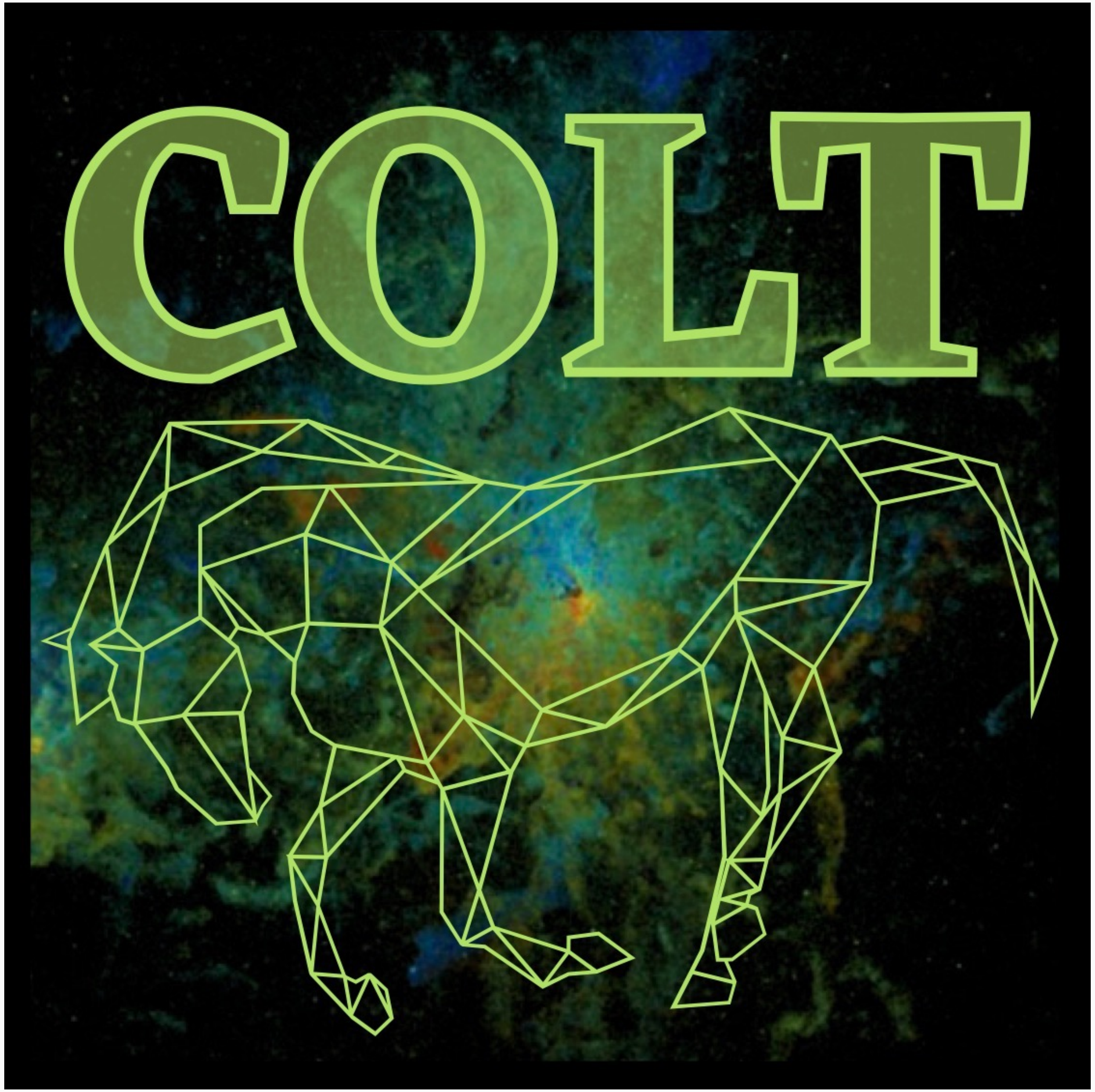

Cosmic Lyα Transfer code

- Monte Carlo Radiative Transfer
- Assortment of Related Tools
- Parallel: MPI + OpenMP
- Geometry: Voronoi, AMR, etc.
- Open source: **colt.readthedocs.io**

Main Applications:

- Accurate treatments of RT
- Probe astrophysics / feedback

Monte Carlo Radiative Transfer for Emission Lines

Recombination: $L_X^{\mathrm{rec}} = h\nu_X \int P_{\mathrm{B},X}(T, n_e)\alpha_{\mathrm{B}}(T)\, n_e n_p \,\mathrm{d}V$

Collisional Excitation: $L_X^{\mathrm{col}} = h\nu_X \int q_{\mathrm{col},X}(T)\, n_e n_{\mathrm{H\,I}} \,\mathrm{d}V$

- ★ Post-processing photoionization equilibrium (MCRT)
- ★ Dust absorption and anisotropic scattering (Weingartner & Draine 2001)
- ★ Collisional ionization, UV background, etc.
- ★ Spatially / spectrally resolved line RT

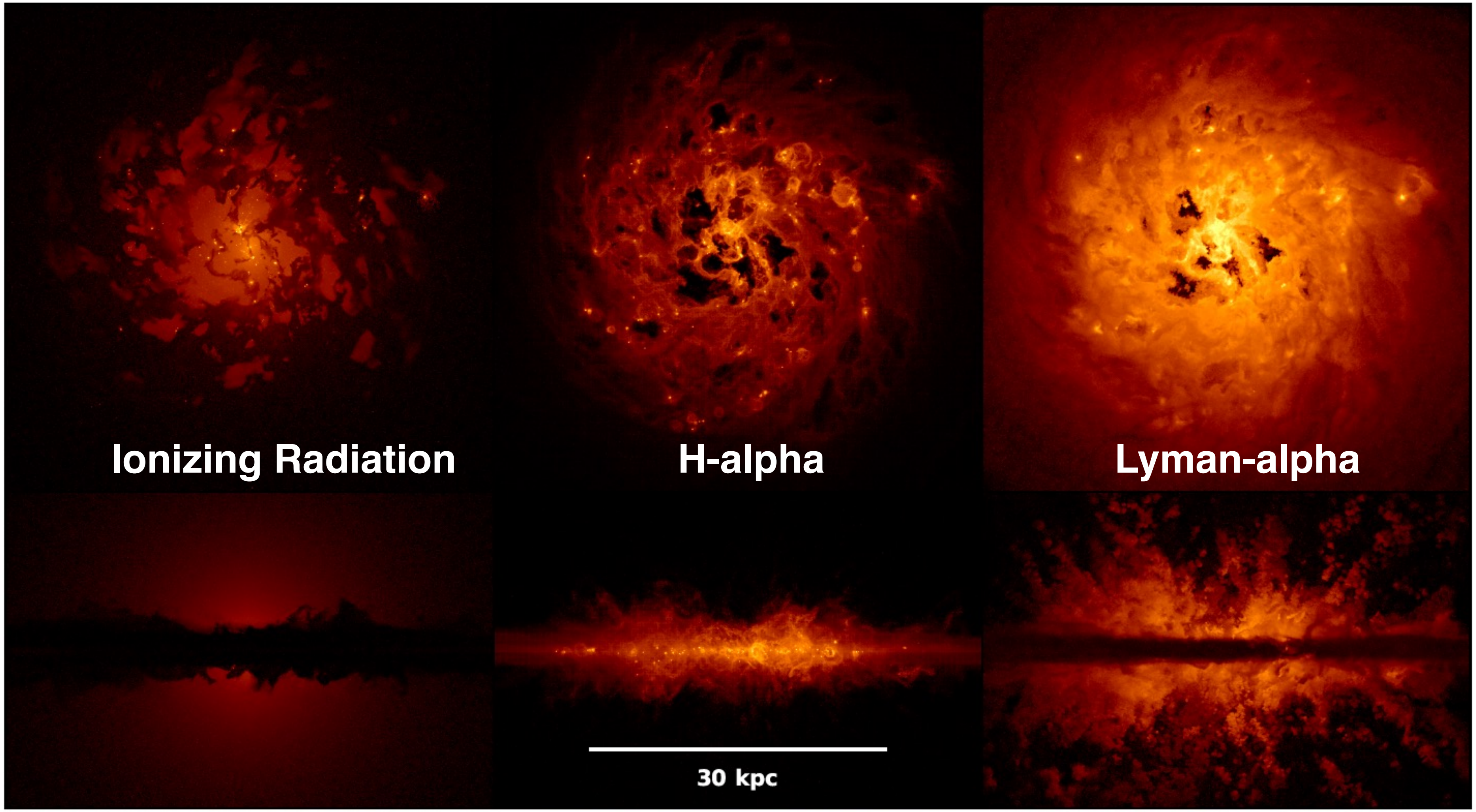

∗ Smith et al. (2022)
∗ Tacchella et al. (2022)

Physical picture of the underlying physics and viewing angle dependence

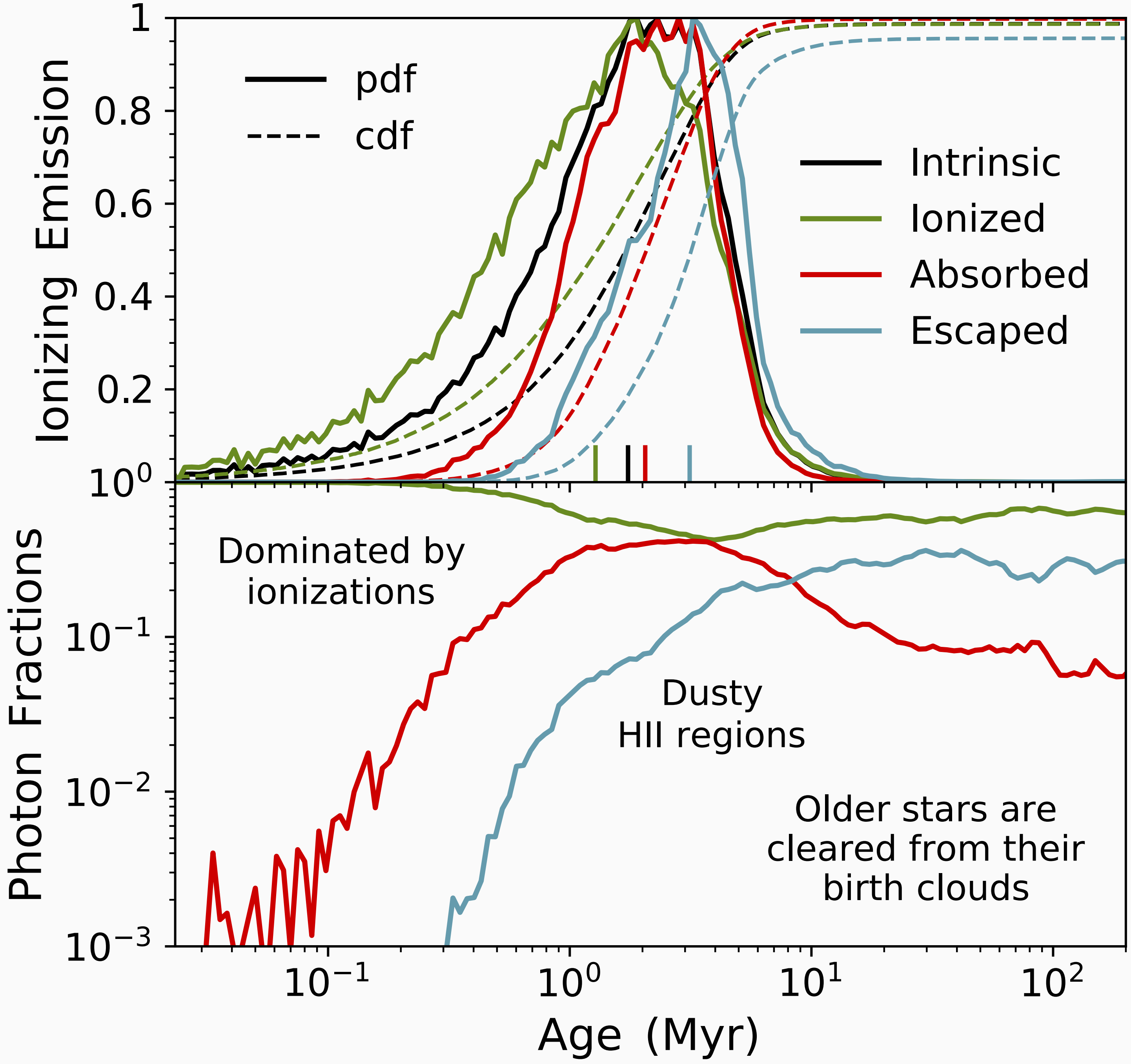

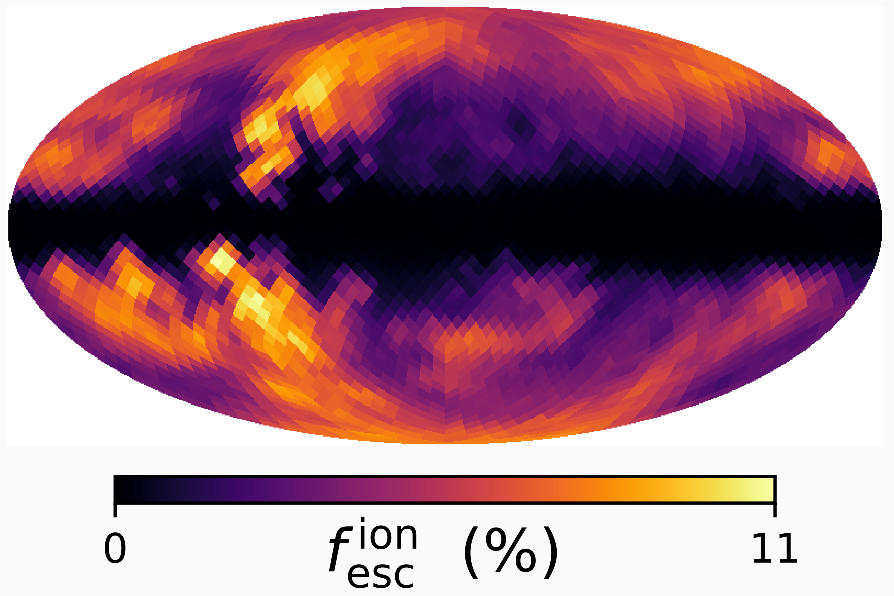

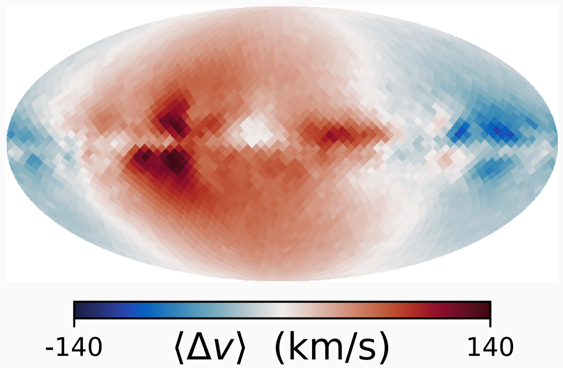

Density and temperature dependence of H-alpha

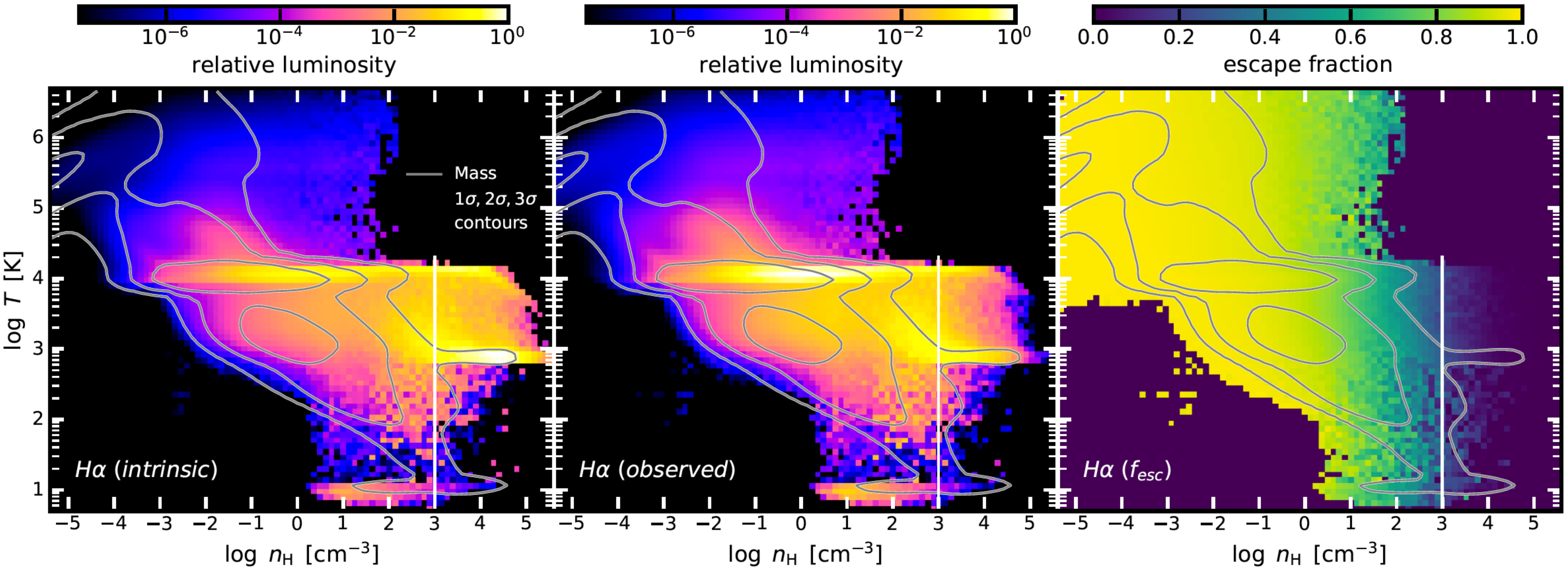

- Most Hα emission comes from dense HII regions with a characteristic temperature of $T \sim 10^4$ K
- The denser the gas, the more pronounced the dust absorption and hence the lower the escape fraction

Comparisons with observations

Hα and Hβ radial profile comparison to SFR-selected sample in MANGA

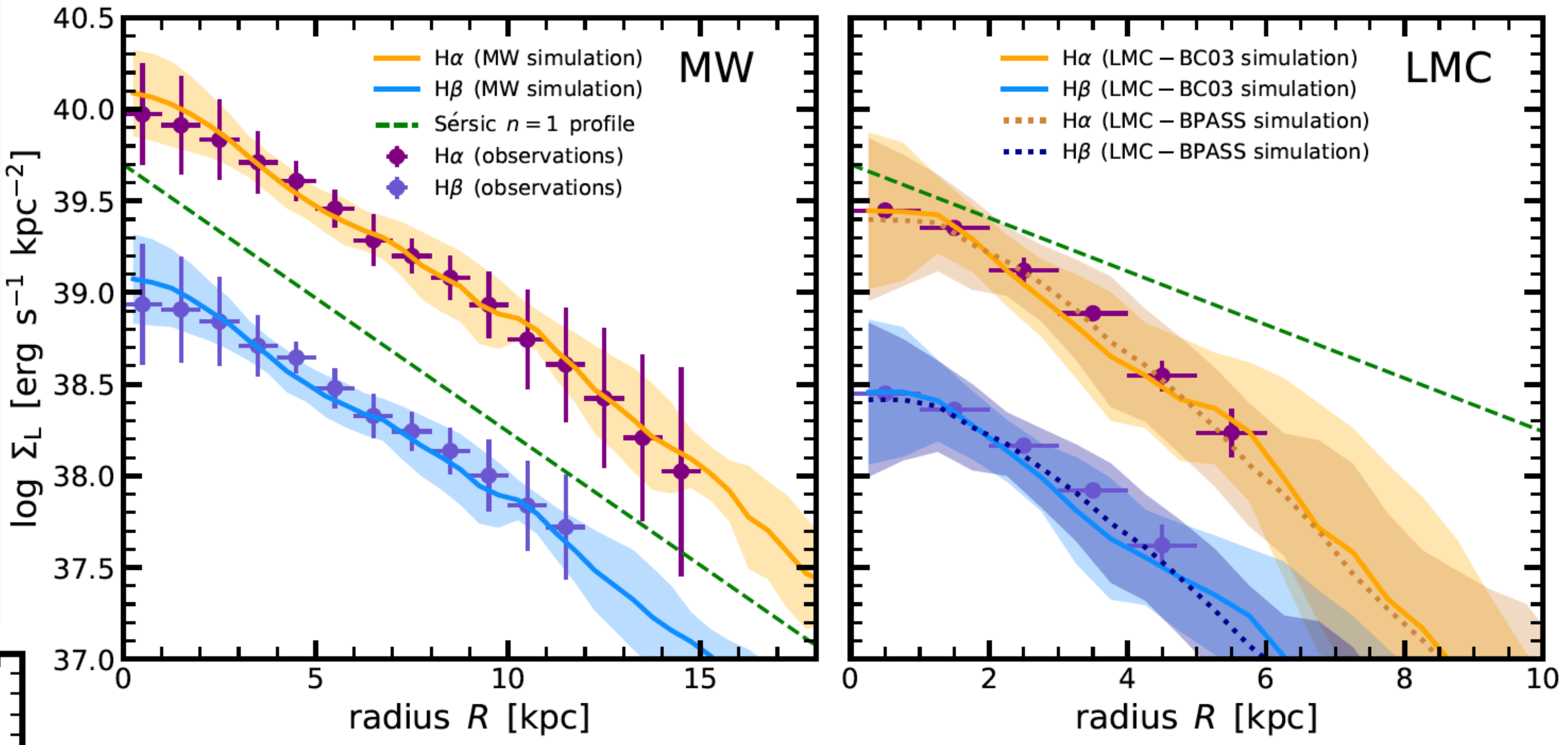

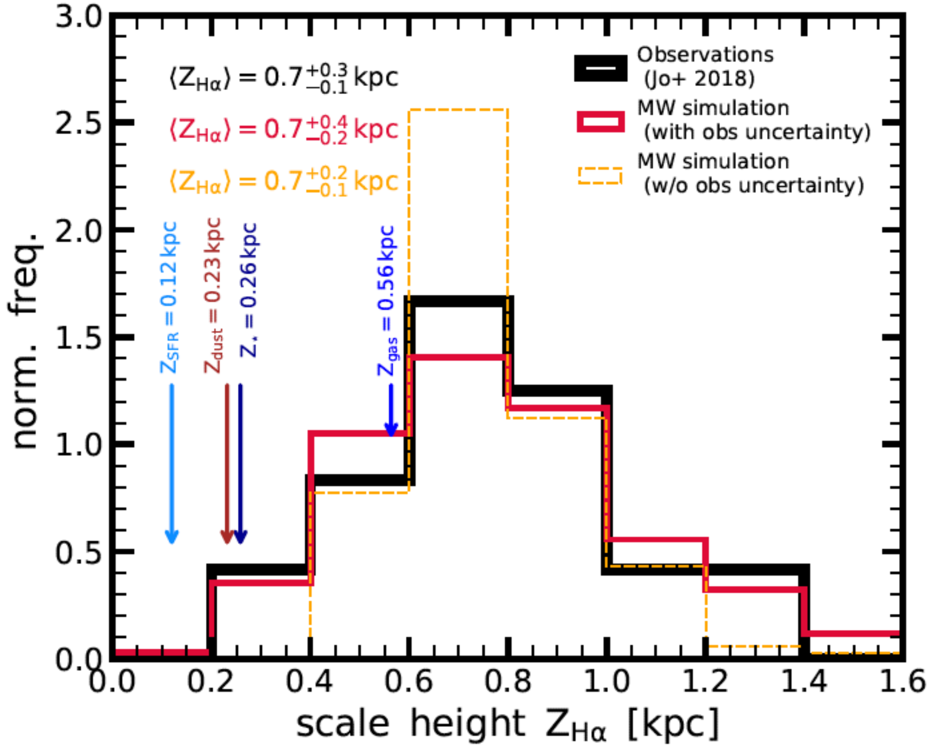

Comparison of H-alpha scale heights of edge-on galaxies

→ Origin of extraplanar Hα emission:

In-situ ionization, i.e. photons transported through pathways carved out by super-bubbles or chimneys rather than significant scattering at high latitudes

Balmer decrement and SFR factor

Hα observed

1 ↓ Dust attenuation correction (Hα/Hβ)

Hα intrinsic

2 ↓ Ha-SFR conversion factor

SFR

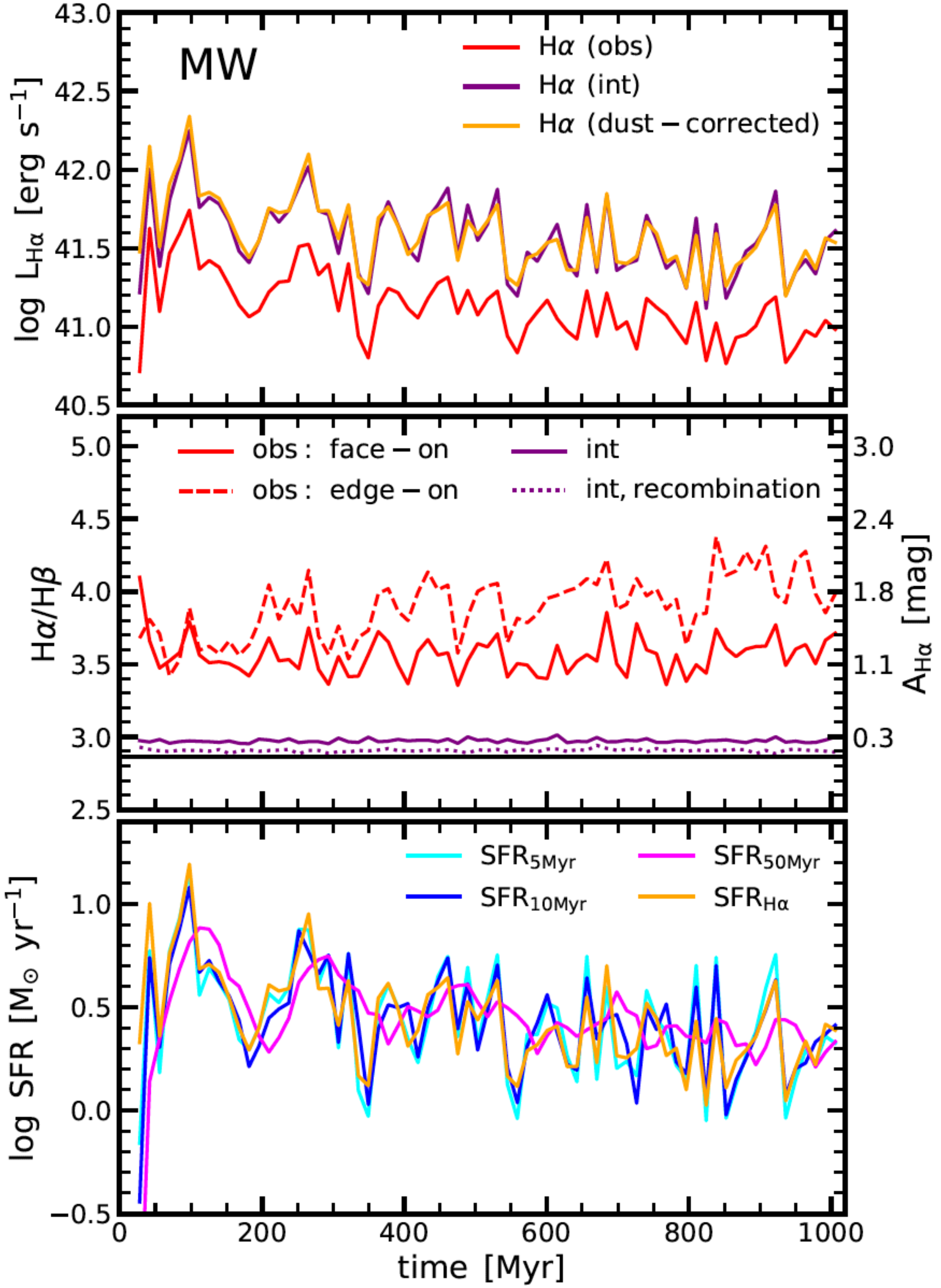

Step 1: Dust correction — observed to intrinsic Hα luminosity

Dust correction via the Balmer decrement:

$$A_{\mathrm{H}\alpha} = \frac{k(\lambda_{\mathrm{H}\alpha})}{k(\lambda_{\mathrm{H}\beta}) - k(\lambda_{\mathrm{H}\alpha})} \times 2.5 \log\left(\frac{(\mathrm{H}\alpha/\mathrm{H}\beta)_{\mathrm{obs}}}{(\mathrm{H}\alpha/\mathrm{H}\beta)_{\mathrm{int}}}\right)$$

But what is the attenuation law k(λ)?
The slope of the attenuation law *n* depends on the attenuation itself, consistent with other RT models (Chevallard et al. 2013) and observations (Salim & Narayanan 2020)
➜ Explained by scattering (red vs. blue light)

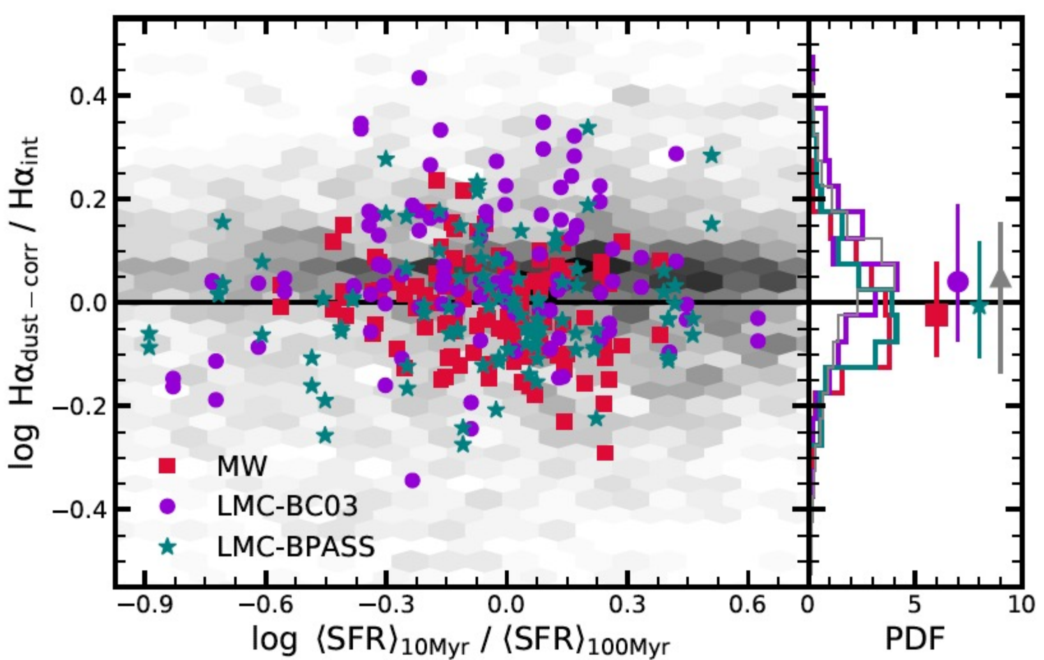

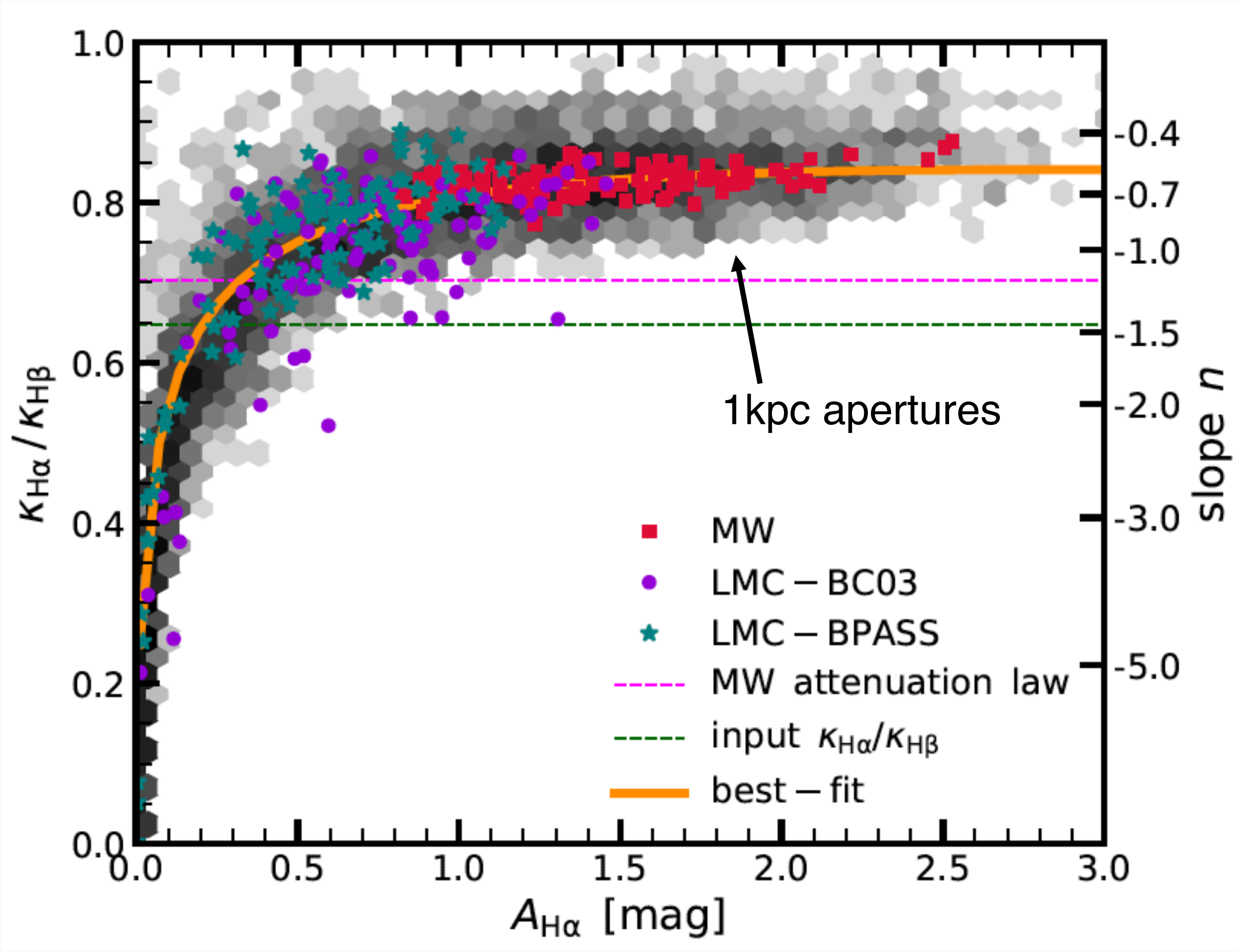

$$\log(\kappa_{\mathrm{H}\alpha}/\kappa_{\mathrm{H}\beta}) = n \log(\lambda_{\mathrm{H}\alpha}/\lambda_{\mathrm{H}\beta})$$
$$= -0.09 \log(A_{\mathrm{H}\alpha})^2 + 0.08 \log(A_{\mathrm{H}\alpha}) - 0.09$$

Balmer decrement works well,
but with > 0.1 dex scatter

Step 2: Intrinsic Hα luminosity to SFR conversion factor

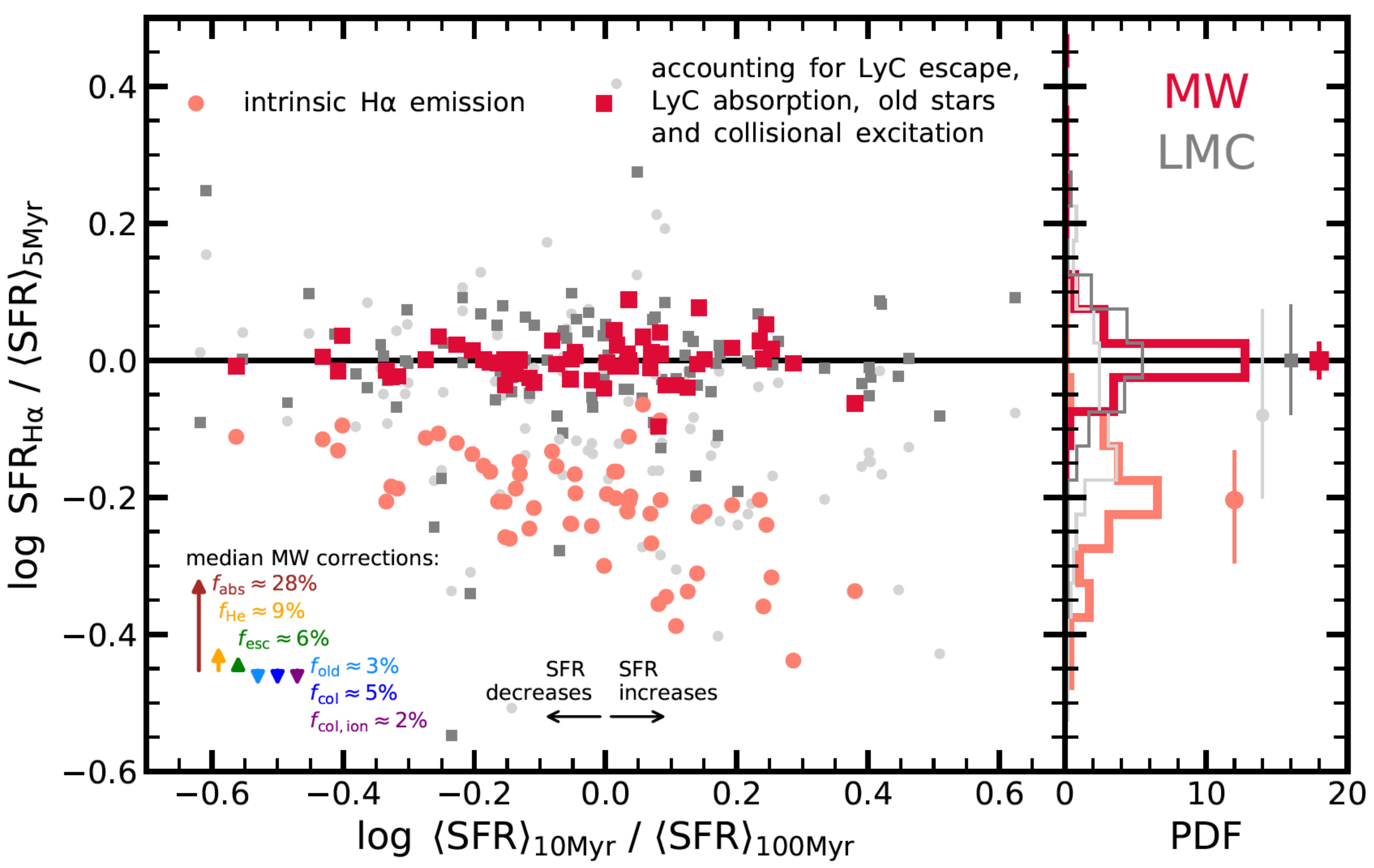

Hα—SFR calibrations need to account for LyC absorption by

- dust ~ 28 %
- Helium ~ 9 %
- escape ~ 6%

Only about 57% available for Hydrogen ionization (matches observations from Inoue+03)

Work in Progress

- **THESAN-Zooms:** Cosmological zoom-in simulations based on the SMUGGLE-RT framework as part of the THESAN project

- The MCRT framework allows us to:
  (i) better understand observations and accurately estimate uncertainties to reveal possible biases
  (ii) gain inspiration for new observational projects

- Extending the MCRT framework to include metal ionization for nebular line studies:
  (i) selection efficiency of diffuse ionized gas (DIG) via the strength of the [SII] emission line
  (ii) understanding how the DIG potentially biases strong-line gas-phase metallicity measurements
  (iii) improved selection of star formation, AGN, and shock regions in galaxies
  (iv) calibrations of ISM pressure and electron density diagnostics (e.g. Kewley et al. 2019)

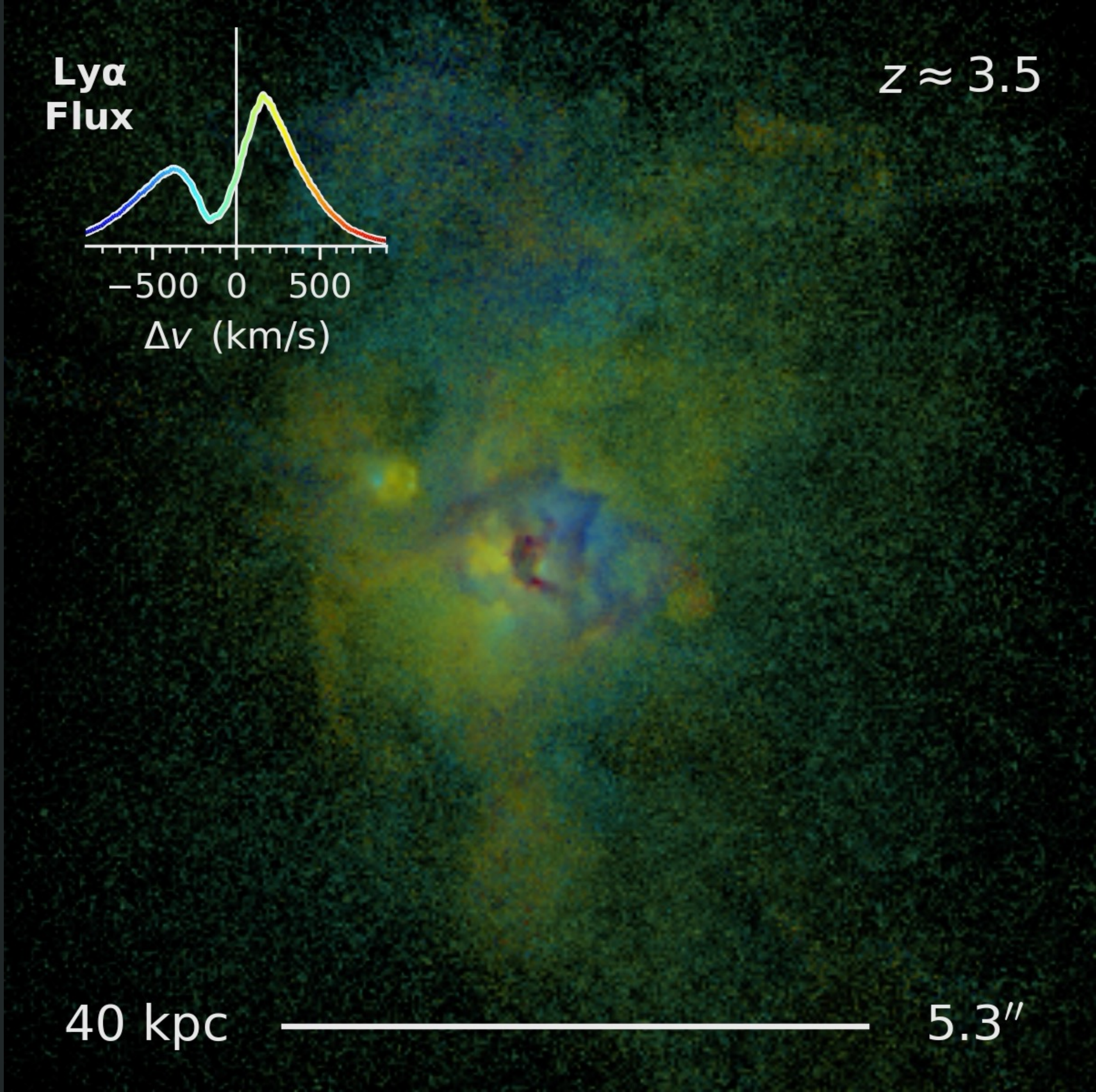

Questions?

★ THESAN data products:

- Full snapshots, FoF catalogs, etc.
- Lyα intrinsic emission for every halo
- Lyα IGM transmission and statistics
- SKIRT spectral energy distributions
- LyC escape fractions and analyses
- Renders for line intensity mapping

★ COLT: Cosmic Lyα Transfer code

- Monte Carlo Radiative Transfer
- Photoionization & emission lines
- Projections, renderings, extractions
- Any geometry: Voronoi, Octree, etc.
- Code is public! **colt.readthedocs.io**

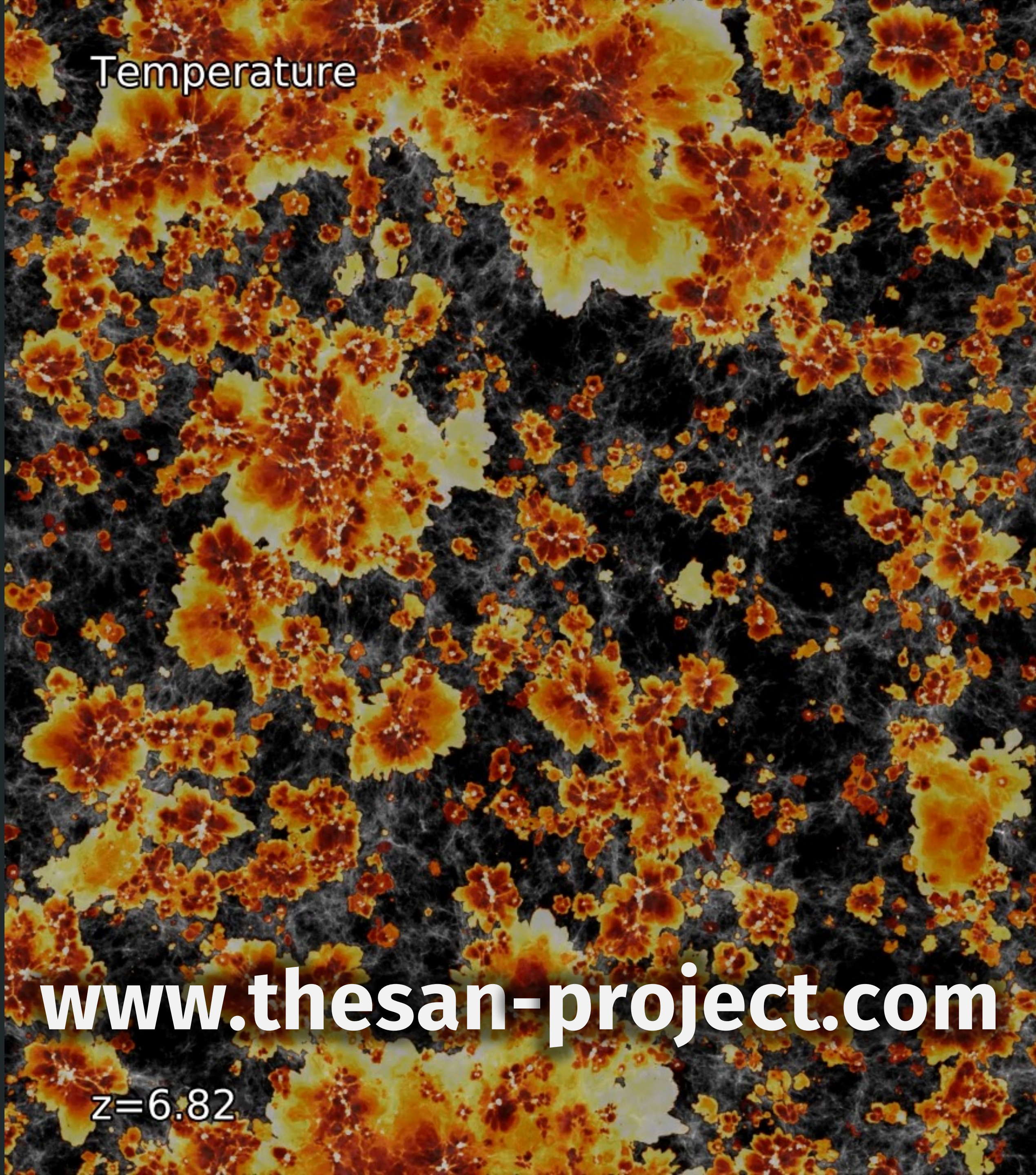

Bonus Slides

In case there is extra time

Updated Treatment of Collisional Excitation for Emission Lines

$$L_X^{\mathrm{col}} = h\nu_X \int q_{\mathrm{col},X}(T)\, n_e n_{\mathrm{H\,I}}\, \mathrm{d}V$$

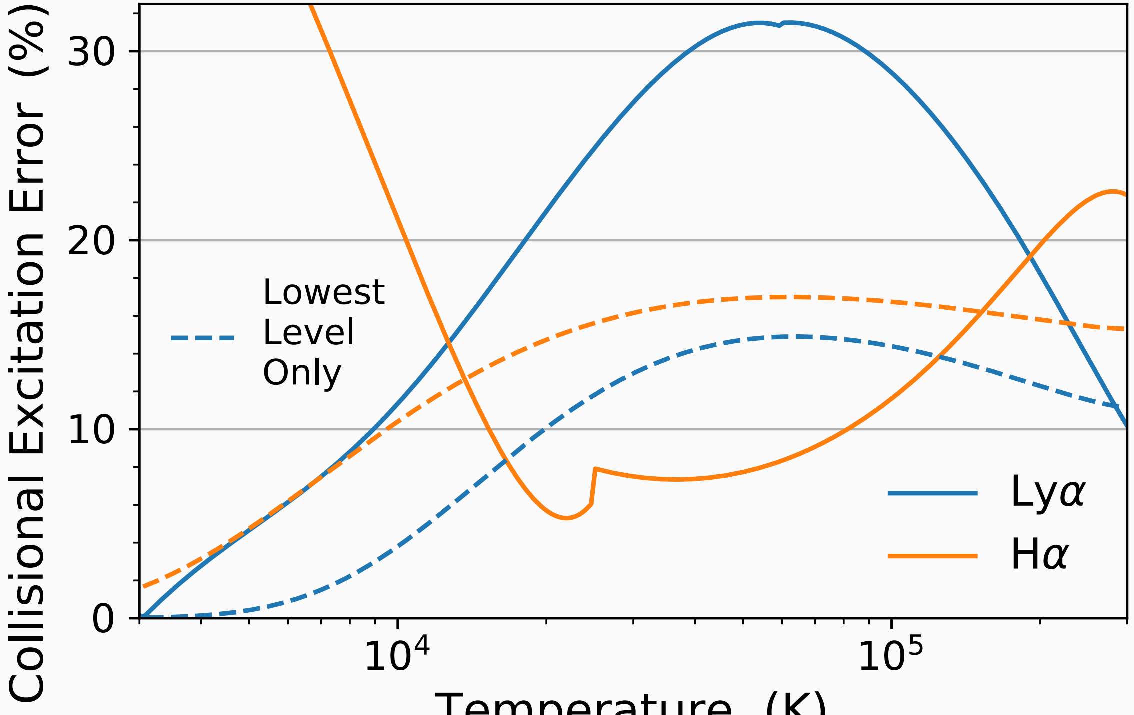

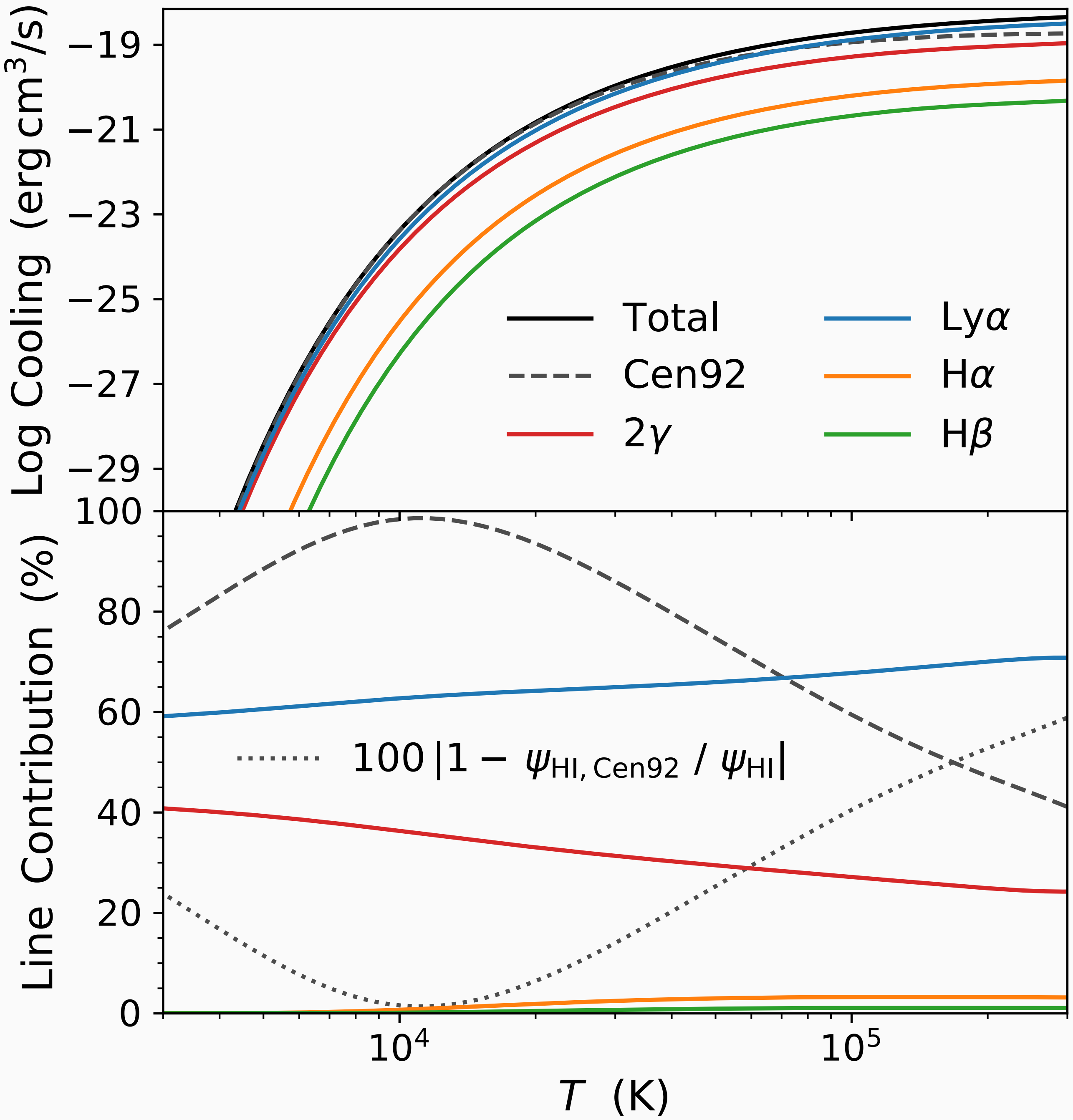

Diffuse Ionized Gas (DIG)

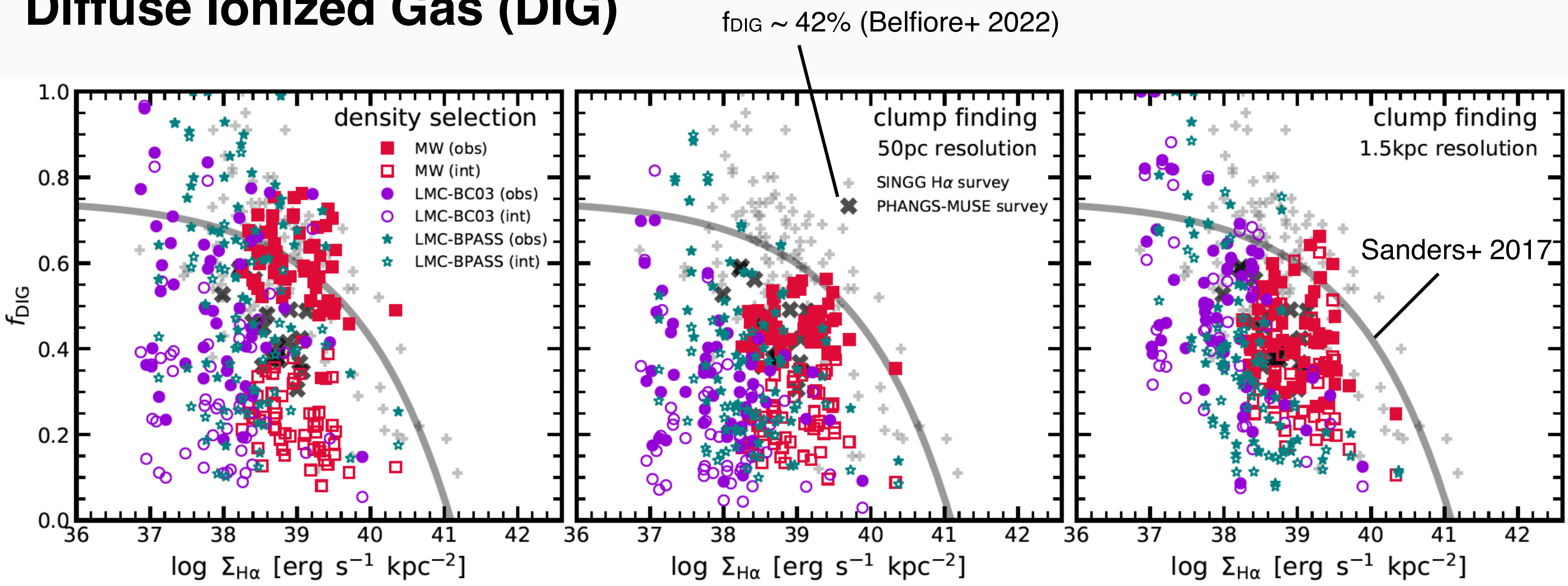

→ intrinsic $f_{\rm DIG}$ is a factor of 2-3 lower than observed $f_{\rm DIG}$

→ $f_{\rm DIG}$ strongly depends on DIG definition

→ BPASS leads typically to higher $f_{\rm DIG}$ than BC03 stellar populations

	density selection		clump finding (50 pc)		clump finding (1.5 kpc)	
Simulation	$f_{\rm DIG,obs}$	$f_{\rm DIG,int}$	$f_{\rm DIG,obs}$	$f_{\rm DIG,int}$	$f_{\rm DIG,obs}$	$f_{\rm DIG,int}$
MW	$0.59^{+0.10}_{-0.08}$	$0.24^{+0.09}_{-0.07}$	$0.44^{+0.08}_{-0.04}$	$0.23^{+0.09}_{-0.07}$	$0.42^{+0.12}_{-0.10}$	$0.37^{+0.11}_{-0.13}$
LMC-BC03	$0.49^{+0.22}_{-0.17}$	$0.26^{+0.21}_{-0.13}$	$0.32^{+0.12}_{-0.13}$	$0.19^{+0.11}_{-0.09}$	$0.50^{+0.18}_{-0.21}$	$0.45^{+0.23}_{-0.19}$
LMC-BPASS	$0.66^{+0.19}_{-0.23}$	$0.39^{+0.23}_{-0.17}$	$0.43^{+0.15}_{-0.17}$	$0.42^{+0.12}_{-0.10}$	$0.37^{+0.32}_{-0.19}$	$0.33^{+0.33}_{-0.18}$

Diffuse Ionized Gas (DIG): EW

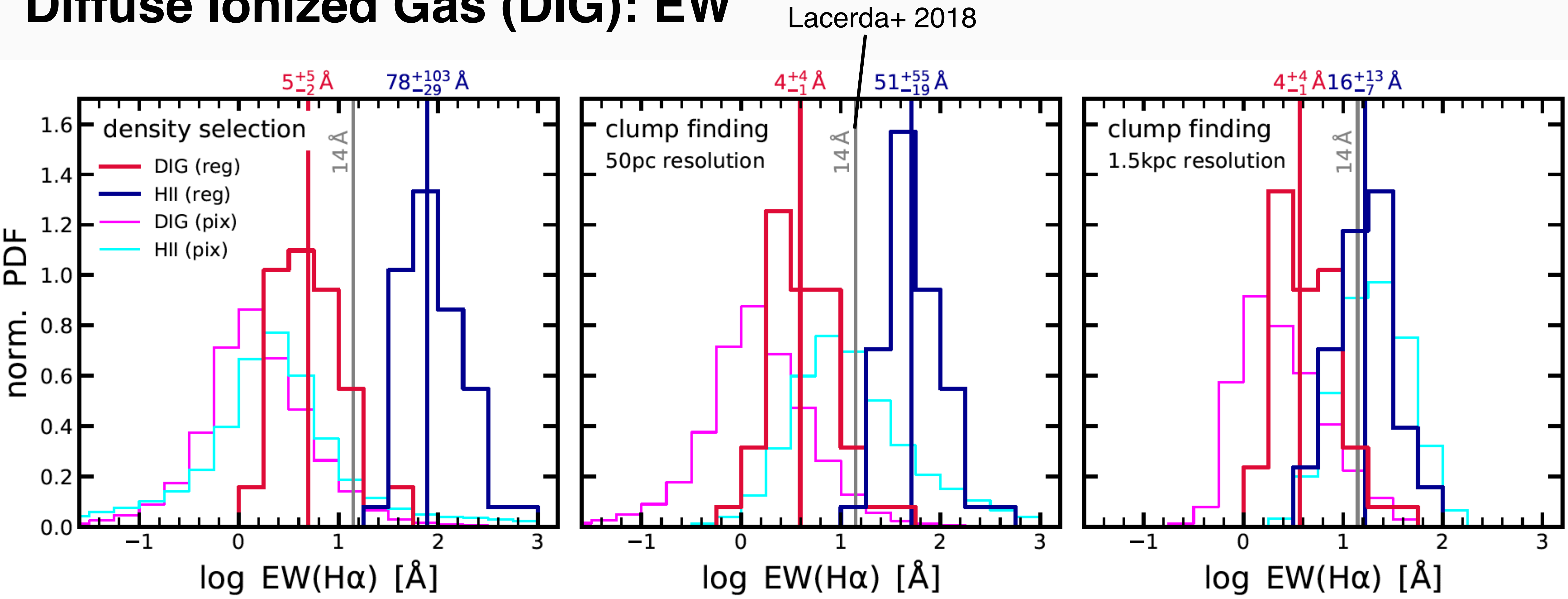

→ EW estimation of DIG and HII regions depend on selection method and binning

→ MUSE observations (Belfiore et al. 2022):
EW(Hα) = $5.3^{+12.1}_{-3.0}$ Å for the DIG and EW(Hα) = 49^{+98}_{-34} Å for the HII regions.

Diffuse Ionized Gas (DIG): What powers the DIG

- in the MW simulation about 30% of all the LyC photons travel 0.01–1.0 kpc before they ionize hydrogen or undergo dust absorption → enough to power an intrinsic DIG fraction of 20–30% as required
- nevertheless, we find that additional processes such as collisional excitation and ionization (related to, e.g., shocks) also contribute to the Hα emission on the 5–10% level
- older stars (>10^8 yr) contribute to ~2% the ionizing budget of the MW simulation and therefore do not dominate the DIG emission

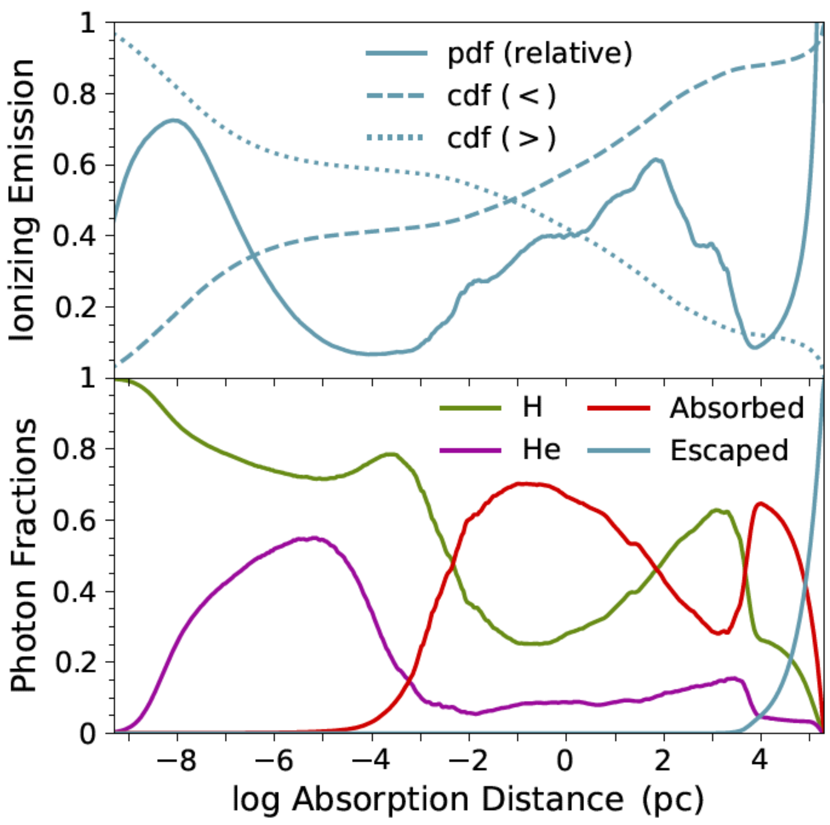

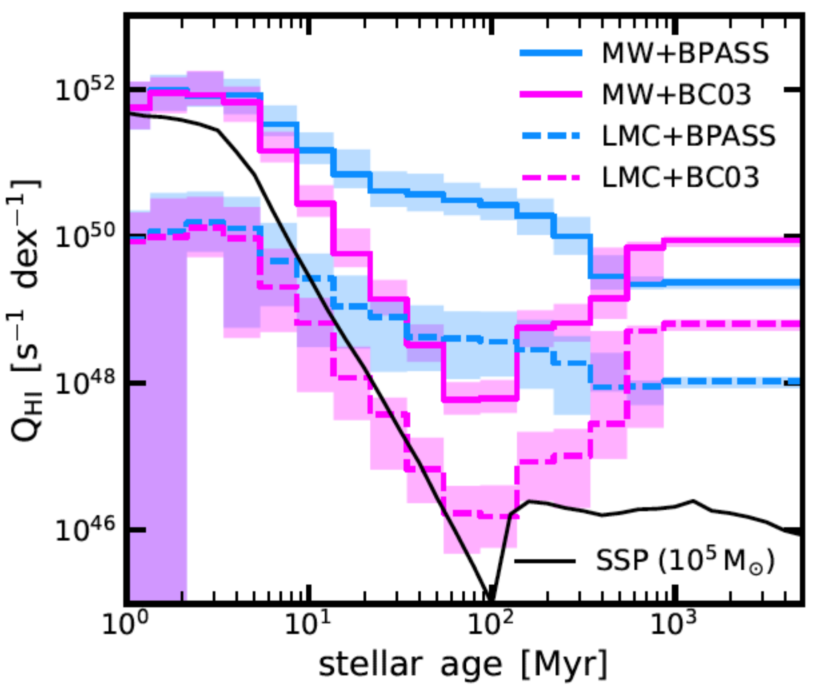

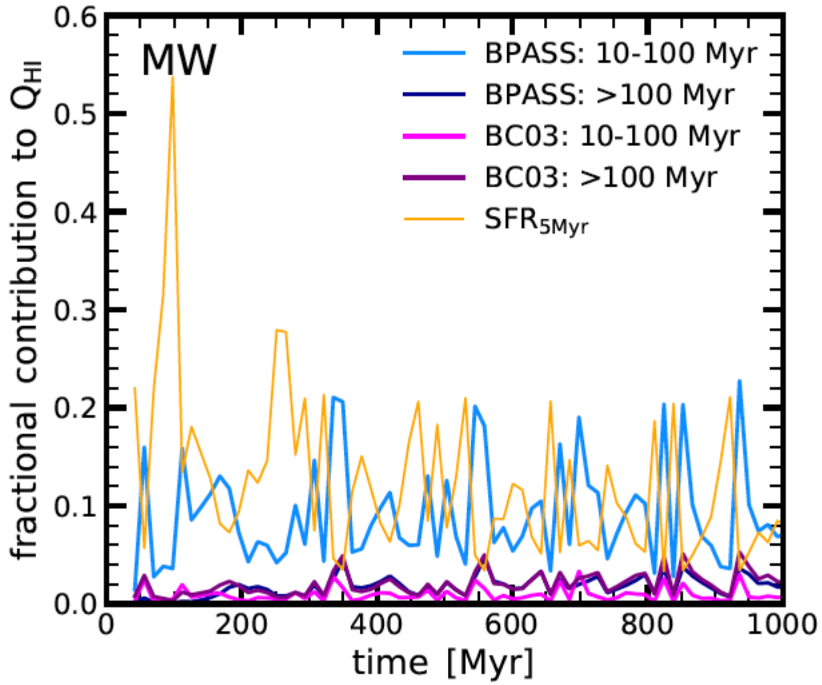

Extraplanar Balmer emission of the MW simulation

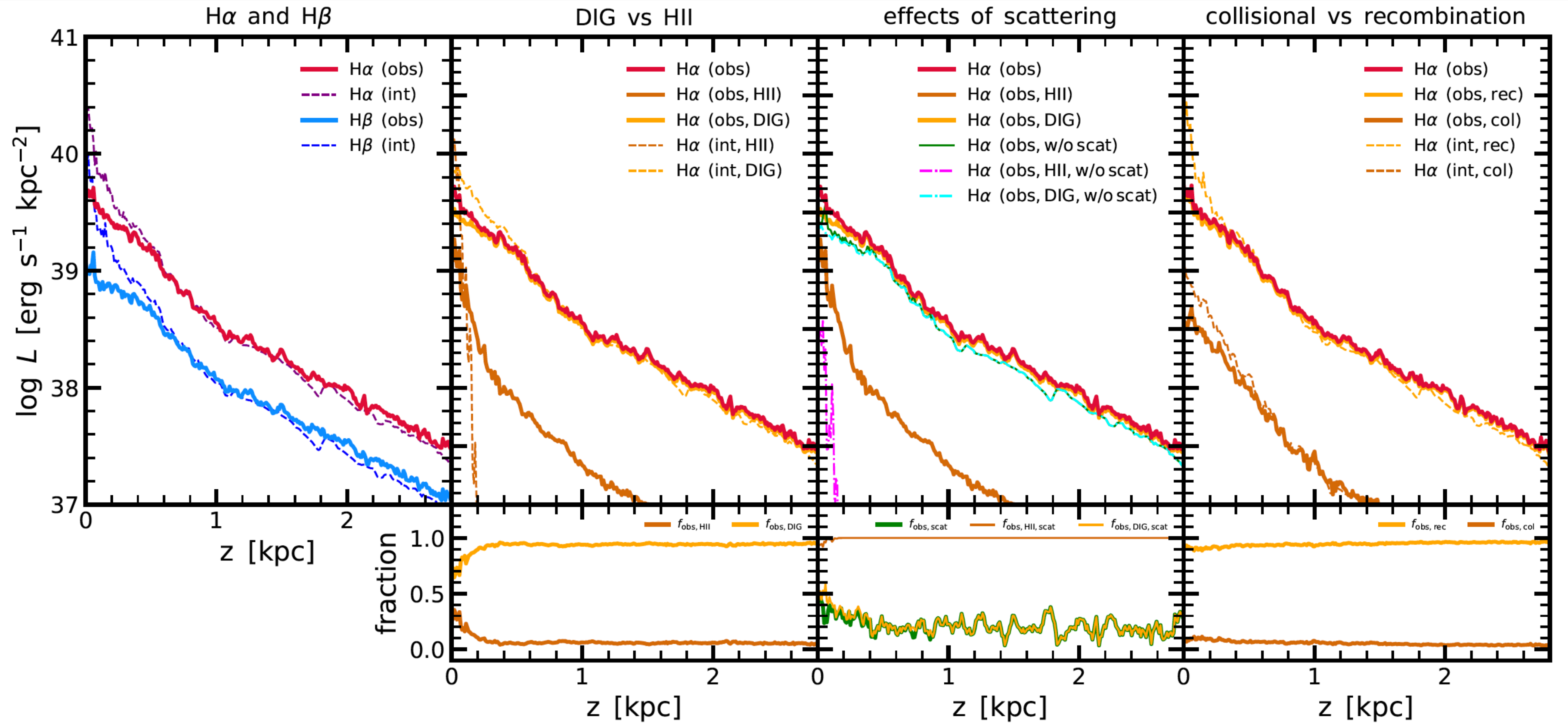

most photons emitted in-situ as DIG

scattering is significant (f_{HII}~100%; f_{DIG}~20%)

recombination dominates over collisional

→ Balmer emission at large scale heights is mainly emitted in-situ via radiative recombination, emitted in low density gas (i.e. the DIG), and scattering is significant but not dominant (f_{scat}≈20%)